



# Sustained effect of zero-valent iron nanoparticles under semi-continuous anaerobic digestion of sewage sludge: Evolution of nanoparticles and microbial community dynamics

Raquel Barrena<sup>a,\*</sup>, María del Carmen Vargas-García<sup>b</sup>, Georgina Capell<sup>a</sup>, Maja Barańska<sup>a</sup>, Victor Puntès<sup>c,d,e</sup>, Javier Moral-Vico<sup>a</sup>, Antoni Sánchez<sup>a</sup>, Xavier Font<sup>a</sup>

<sup>a</sup> GICOM research group, Department of Chemical, Biological and Environmental Engineering, Universitat Autònoma de Barcelona, Edifici Q, Carrer de les Sitges, 08193 Bellaterra (Cerdanyola del Vallès), Barcelona, Spain

<sup>b</sup> Department of Biology and Geology, CITE II-B, Universidad de Almería, Agrifood Campus of International Excellence ceia3, 04120 Almería, Spain

<sup>c</sup> Catalan Institute of Nanoscience and Nanotechnology (ICN2), CSIC and BIST, Campus UAB, Bellaterra, 08193 Barcelona, Spain

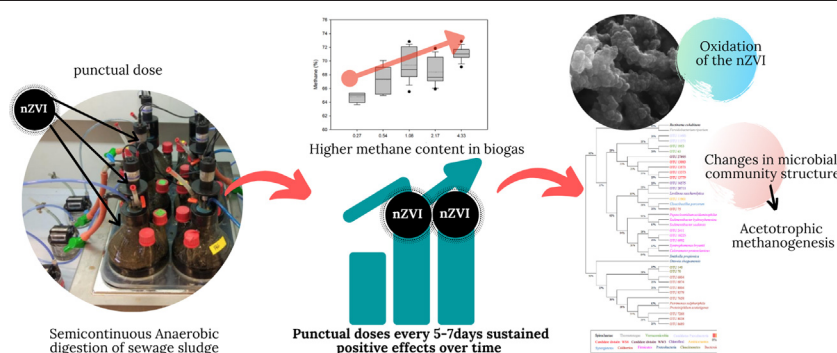
<sup>d</sup> Vall d'Hebron Institut de Recerca (VHIR), 08035 Barcelona, Spain

<sup>e</sup> Institutió Catalana de Recerca i Estudis Avançats (ICREA), P. Lluís Companys 23, 08010 Barcelona, Spain

## HIGHLIGHTS

- Dosing of nZVI improved methane content in the anaerobic digestion.
- Punctual doses every 5–7 days sustained positive effects with higher methane content.
- Magnetic retention of nZVI in reactors showed the loss of effect along time.
- TEM-EELS analysis showed the oxidation of nZVI during anaerobic digestion.
- Changes in microbial community structure can be related to nZVI use.

## GRAPHICAL ABSTRACT



## ARTICLE INFO

### Article history:

Received 17 November 2020

Received in revised form 12 February 2021

Accepted 13 February 2021

Available online 19 February 2021

Editor: Damia Barcelo

### Keywords:

nZVI

Anaerobic digestion

*Methanotrix*

Oxidation state

Magnetic nanoparticles

## ABSTRACT

The effects of adding zero-valent iron nanoparticles (nZVI) on the physicochemical, biological and biochemical responses of a semi-continuous anaerobic digestion of sewage sludge have been assessed. Two sets of consecutive experiments of 103 and 116 days, respectively, were carried out in triplicate. nZVI were magnetically retained in the reactors, and the effect of punctual doses (from 0.27 to 4.33 g L<sup>-1</sup>) over time was studied. Among the different parameters monitored, only methane content in the biogas was significantly higher when nZVI was added. However, this effect was progressively lost after the addition, and in 5–7 days, the methane content returned to initial values. The increase in the oxidation state of nanoparticles seems to be related to the loss of effect over time. Higher dose (4.33 g L<sup>-1</sup>) sustained positive effects for a longer time along with higher methane content, but this fact seems to be related to microbiome acclimation. Changes in microbial community structure could also play a role in the mechanisms involved in methane enhancement. In this sense, the microbial consortium analysis reported a shift in the balance among acetogenic eubacterial communities, and a marked increase in the relative abundance of members assigned to *Methanotrix* genus, recognized as acetoclastic species showing high affinity for acetate, which explain the rise in methane content in the biogas. This research demonstrates that biogas methane enrichment in semicontinuous anaerobic digesters can be achieved by using nZVI nanoparticles, thus increasing energy production or reducing costs of a later biogas upgrading process.

© 2021 The Authors. Published by Elsevier B.V. This is an open access article under the CC BY-NC-ND license (<http://creativecommons.org/licenses/by-nc-nd/4.0/>).

\* Corresponding author.

E-mail address: [raquel.barrena@uab.cat](mailto:raquel.barrena@uab.cat) (R. Barrena).

## 1. Introduction

High world energy demand and waste generation conflict with biosphere preservation. Thus, the transition from fossil fuels to renewable energy sources, along with the improvement of solid waste treatment, becomes a necessary changeover for the balance between humankind and the environment. In this context, anaerobic digestion (AD) is a well-implemented technology to treat a wide range of organic waste streams, such as livestock manure, domestic and industrial wastewaters, food waste, or fat and oils (Lora Grando et al., 2017) while producing green energy. Through the implementation of AD, an energetically optimal product, *biogas*, a mixture of methane (CH<sub>4</sub>) and carbon dioxide (CO<sub>2</sub>), is obtained. Nevertheless, the AD process still needs to be optimized to bring more and better-quality energy. The use of additives to increase biogas production and the improvement of biogas upgrading are among the aspects that can still promote the advancement of AD (Lora Grando et al., 2017).

Iron is recognized as a potential energy source for bacteria. It is an essential redox element (between Fe<sup>2+</sup> and Fe<sup>3+</sup> forms) fundamental for biological processes that functions as a versatile cofactor for numerous proteins in biological processes. It plays a fundamental role in biological processes such as DNA replication and repair among others, but also as an electron donor and acceptor in many microorganisms such as Archae and Bacteria (Folgora et al., 2015). Although iron is one of the most abundant elements on earth, its bioavailability is not as extensive as it would be expected, since at neutral pH its solubility is 0.1 M and 10<sup>-8</sup> M, for Fe<sup>2+</sup> and Fe<sup>3+</sup>, respectively. The optimal proportion of trace metal could be a crucial aspect of the AD process (Baniamerian et al., 2019), and thus, their supplementation can be a powerful tool. Casals et al. (2014) indicated that the key to maintaining the increased biogas production was to preserve an optimal iron concentration in an anaerobic digester over time.

The use of nanoparticles (NPs) as new additives in AD is an emerging technology, especially explored in the last years (Baniamerian et al., 2019). Nanoscale zero-valent iron (nZVI) can be found among the studied nanomaterials. Thanks to their characteristics, nanoscale zero-valent metals are expected to have more promising applications compared to their bulk counterparts (Baniamerian et al., 2019). Recent studies have proven that nZVI could be an effective additive to enhance AD of sewage sludge, especially the increase of methane content in the biogas (Córdova et al., 2019; Su et al., 2013). The positive results of nZVI addition have been related both, to the enhancement of enzyme activities in hydrolysis and acidification steps (Zhang et al., 2020) even during the removal of persistent organic substances in waste activated sludge (Zhou et al., 2020) and antibiotics (Zhou et al., 2021); and the growth of H<sub>2</sub>-utilizing microorganisms including homoacetogens and hydrogenotrophic methanogens by providing electrons directly or producing hydrogen through the iron anaerobic oxidation (Zhen et al., 2015; Xu et al., 2019). However, adverse effects on the methanogenesis were also reported at high doses (Dong et al., 2019). Some references using powder and scrap Fe in AD experiments have shown positive effects in biogas yield. However, although Fe<sup>0</sup> has been reported to improve hydrolysis–acidification and the CH<sub>4</sub> yield, its efficiency was low compared with nZVI (Wang et al., 2018) because it is directly proportional to its specific surface area. Instead, other authors did not observe any effect using micro-scale zero-valent iron (200 μm) (Xu et al., 2019).

In a moment when some research efforts are focused on the upgrading of biogas or broaden its applications, the use of nanoparticles can be a promising way to have enriched methane streams of biogas. In this case, the residual CO<sub>2</sub> of these streams can be further removed using novel and consolidated techniques (adsorption, absorption, membranes, etc.). Although some studies have evaluated the effects of nZVI on AD of sewage sludge, their application in a more realistic continuous process has been scarcely explored, a fact that could imply changes from those effects observed in batch conditions. It is expected that the addition of nZVI increases methane production in (semi)realistic conditions

and also that their presence change the microbial profile towards more methane-generating microbial communities. Specifically, this work aims to assess the effects of nZVI punctually dosed at different concentrations and different interval in a semi-continuous operation and establish an operation mode that sustains the positive effects but avoids a continuous and extra NPs addition. With that purpose, nZVI were magnetically retained in the reactors, and the effect of punctual doses over time was studied. Different doses were tested to study both the impact on methane production and their persistence over time. The oxidation state of nZVI and the microbial community dynamics after nZVI addition was also addressed to understand: i) the loss of nZVI effect on methane production over time ii) the acclimation and adaptation of microorganisms to nZVI.

## 2. Materials and methods

### 2.1. Synthesis and characterization of nZVI

nZVI were synthesized following the protocol proposed by Choe et al. (2001). To obtain 6.5 g L<sup>-1</sup> of Fe<sup>0</sup>, 7.04 g of NaBH<sub>4</sub> (≥98%) were dissolved in 200 mL of deoxygenated ultrapure water and then added dropwise to 200 mL of a deoxygenated FeCl<sub>3</sub> (≥98%) 7.54 g L<sup>-1</sup> solution. After 25 min of vigorous stirring under an N<sub>2</sub> atmosphere, the Fe<sup>0</sup> precipitate was rinsed three times with deoxygenated ultrapure water to remove residual acidity or impurities, redispersed in 400 mL of ultrapure water and finally stored in a 500 mL glass bottle after flushing N<sub>2</sub>. NPs suspension was ultrasonicated for 30 min before every use to avoid agglomeration. All chemicals were purchased from Sigma-Aldrich and used as received.

nZVI were characterized in terms of size, distribution and morphology by scanning electron microscopy (SEM), using a Quanta FEI 200 FEG-ESEM instrument, equipped for energy-dispersive X-ray analysis (EDX). Electron energy-loss spectroscopy in a transmission electron microscope (TEM-EELS) analysis for the determination of the oxidation state of NPs was performed on an FEI Tecnai G2 F20 microscope equipped with a Gatan Imaging Filter (GIF) Quantum SE 963 operating at 200 kV.

### 2.2. Inoculum and substrate

Anaerobic sludge used as inoculum and was obtained from the mesophilic anaerobic digester of Riu Sec municipal wastewater treatment plant (WWTP) (Sabadell, Barcelona, Spain). Sewage sludge fed daily to the reactors was also collected from the Riu Sec WWTP. The sludge was collected periodically, twice for Experiment 1 (3.7% total solids TS); 2.7% volatile solids (VS) and 3.3% TS; 1.8% VS and once for Experiment 2 (3.7% TS; 2.9% VS) and stored in 0.5-L plastic bottles at a temperature of -24 °C and thawed at room temperature when used.

### 2.3. Anaerobic digestion experimental set-up and procedure

The experimental set-up consisted of six fermentation glass vessel reactors used in two sets of semi-continuous operation of 103 days (Experiment 1) and 116 days (Experiment 2). The reactors were operated at 37 °C with intermittent stirring: agitated for 15 min every 45 min using a mixing device located on the top. The total volume for each reactor was 2 L (1.8 L working volume). The hydraulic retention time (HRT) was set at 21 days, as it was in Riu Sec WWTP, following a semi-continuous feeding strategy, according to which the reactors were fed manually once a day, 5 days a week (from Monday to Friday) replacing the same volume that was previously extracted from them. The substrate feeding/exchange was done as follows: during the agitation period, 80 mL of digestate were extracted by using a graduated 50 mL syringe through the outlet pipe. Then, 80 mL of new feed was introduced in the reactors through the inlet pipe. After feeding, all reactors were flushed with N<sub>2</sub> and then sealed.

The different doses of nanoparticles were added to three reactors (nZVI reactors) while the remaining three were used as control reactors (control reactors). When added, nZVI were fed at the same time that sewage sludge. It is important to note that reactors were fed daily but nZVI were added punctually. Thus, during the daily substrate feeding, nZVI (added the previous days) were retained in the reactors by using a neodymium permanent magnet (NdFeB magnet). The strong magnetic power of the NdFeB maintains in the reactor the main part of nZVI added. The volume of biogas produced was measured by connecting to each reactor a Ritter MilliGascounter (Ritter, Germany). The biogas production was weekly averaged and calculated in reference to the reactor working volume. The process was started-up in the 6 reactors feeding only the sewage sludge during approximately two HRTs before adding the first dose of nZVI.

#### 2.4. nZVI dosing

Different nZVI doses were tested during the semi-continuous AD operation. Table 1 summarizes the punctual doses studied and the day of addition for both experiments. Two sets of experiments were carried out: for Experiment 1, the first dose of nZVI was  $0.27 \text{ g L}^{-1}$  (equivalent to  $10.0 \text{ g kg}^{-1} \text{ SV}$  for Experiment 1 and  $9.3 \text{ g kg}^{-1} \text{ SV}$  for Experiment 2) based on previous works (Casals et al., 2014) and results from a series of batch experiments (Fig. S1) and added on day 38. The second dose was set at  $0.54 \text{ g L}^{-1}$ , doubling the previous one. Later, four more doses of  $0.27 \text{ g L}^{-1}$  were added to the reactors approximately every 7 days from day 74 until 98. Lastly, the dose was increased up to  $0.81 \text{ g L}^{-1}$  to check the system response to higher doses and was supplied on day 99. After the results obtained in Experiment 1, a new process (Experiment 2) was carried out in order to evaluate the effects of incremental doses of nZVI on methane production. Thus, experiment 2 corresponds to a new experiment where the reactors were started-up again with a new inoculum, and after approximately two HRTs the first dose of nZVI was added on day 38. Here, the first punctual dose applied was also  $0.27 \text{ g L}^{-1}$  and then the dose was doubled every time: 0.54, 1.08, 2.17, and  $4.33 \text{ g L}^{-1}$  to see the overall performance of the system under an exponentially increasing dose of nZVI to have preliminary values of the limits of nZVI application.

#### 2.5. Analytical methods

Alkalinity, pH, and volatile fatty acids (VFA) were also periodically evaluated to assess the stability of the process. Total alkalinity (TA) and partial alkalinity (PA), total (TS) and volatile (VS) solids content and pH were determined according to standard methods (APHA, 1999). The intermediate alkalinity (IA) was calculated as the difference between TA and PA. Alkalinity and pH were measured twice a week in a

filtered supernatant sample using a pH-meter (pH 50+ DHS, XS Instruments, Italy). TS and VS were analysed two–three times per week. VFA, specifically formic, acetic, propionic, iso-butyric, butyric, iso-valeric and valeric acids, were measured once a week. VFA samples, filtered through a  $0.22 \mu\text{m}$  polyethersulfone syringe filter (Millipore Millex-GP), were quantified by liquid chromatography (HPLC, Dionex Ultimate 3000) equipped with a 210 nm ultraviolet detector and a Transgenomic ICE-COREGEL 87H3 column ( $300 \text{ mm} \times 4.6 \text{ mm}$ ). The mobile phase consisted of an acid solution of  $320 \mu\text{L L}^{-1}$  of sulphuric acid. The total time for each run was 150 min. A volatile free acid mix solution (CRM46975, Sigma-Aldrich) was used as standard.

Biogas composition was analysed by gas chromatography (GC, Agilent 7820) equipped with a thermal conductivity detector (TCD) and two columns (Agilent G3591-81136 and G3591-80017) connected with a valve and activated with synthetic air. A sample of  $100 \mu\text{L}$  was collected from a valve in the headspace reactors with a gas-tight syringe and injected. Nitrogen was used as carrier gas. Injector and detector temperatures were  $200 \text{ }^\circ\text{C}$  and  $250 \text{ }^\circ\text{C}$ , respectively. The initial oven temperature was  $70 \text{ }^\circ\text{C}$  for 2 min, with a subsequent temperature ramp of  $20 \text{ }^\circ\text{C}$  per minute, up to  $40 \text{ }^\circ\text{C}$  until the end of the analysis. The total time for each run was 6 min. An external standard (100%  $\text{CH}_4$ ) was used for the quantification of  $\text{CH}_4$  content.

#### 2.6. Microbial community analysis

The microbiome was analysed in Experiment 1 from samples extracted from each reactor (total six samples: three from nZVI and control reactors respectively) at end of the study (day 99). Sequencing and bioinformatics were performed by Life Sequencing S.A. (Valencia, Spain). PowerSoil™ DNA Isolation kit (MoBio Laboratories Inc., Carlsbad, CA, USA) was used for the extraction of DNA according to the manufacturer's instructions and extracts were tested to ensure concentration and quality using a NanoDrop™ 2000 spectrophotometer (Thermo Fisher Scientific, Waltham, MA, USA) for the determination of A260/A280 and A260/A320 ratios. Genomic libraries from the V3-V4 hypervariable region 16s rRNA gene were constructed using the universal primers Pro314F (CCTACGGGNBGCASCAG) and Pro805R (GACTACNVGGGTATCTAATCC), designed for the simultaneous detection of Bacteria and Archea (Takahashi et al., 2014). Sequencing data obtained from the Illumina MiSeq platform (Illumina, Inc., San Diego, CA, USA) were analysed according to a 300 bp fragments paired-end protocol and processed using PEAR software v.0.9.1, CUTADAPT software v.1.8.1 and Chimera Uchime (Edgar et al., 2011) for the construction of the overlapped sequences, the removal of adapters and chimeric sequences, respectively. The remaining sequences were examined to select those displaying quality scores higher than Q20 and length > 200. Finally, the CD-HIT software v.4.6.8 was applied for clustering, using a

**Table 1**

Summary of the doses applied and main results from semi-continuous anaerobic digestion processes in Experiment 1 and 2. Different letters in the same column indicate significant differences between the evaluated doses ( $p < 0.05$ ).

Dose ( $\text{g L}^{-1}$ )	Day of addition	Averaged $\text{CH}_4$ (control) (%)	Averaged $\text{CH}_4$ (nZVI)* (%)	Maximum $\text{CH}_4$ (nZVI) (%)	Persistence of improvement (days)*
<b>Experiment 1</b>					
0.27	38	$66.1 \pm 1.8 \text{ a}$	$68.2 \pm 3.0 \text{ a}$	72.6	5
0.54	57	$64.6 \pm 1.7 \text{ a}$	$66.0 \pm 2.3 \text{ a}$	69.3	7
0.27	74	$65.1 \pm 2.1 \text{ a}$	$67.9 \pm 2.8 \text{ a}$	72.1	All (5)
0.27	79	$65.9 \pm 1.6 \text{ a}$	$72.1 \pm 2.6 \text{ b}$	75.1	All (6)
0.27	85	$66.0 \pm 1.9 \text{ a}$	$72.7 \pm 1.7 \text{ b}$	75.4	All (6)
0.27	92	$66.4 \pm 1.0 \text{ a}$	$71.5 \pm 1.8 \text{ b}$	74.0	All (7)
0.81	99	$65.1 \pm 1.5 \text{ a}$	$75.9 \pm 2.8 \text{ c}$	79.2	All (4)
<b>Experiment 2</b>					
0.27	38	$62.1 \pm 1.4 \text{ a}$	$64.8 \pm 0.8 \text{ a}$	65.3	5
0.54	54	$63.2 \pm 1.8 \text{ a}$	$67.3 \pm 2.1 \text{ b}$	70.1	5
1.08	65	$63.8 \pm 2.6 \text{ a}$	$69.4 \pm 2.3 \text{ b}$	72.8	9
2.17	85	$64.0 \pm 1.7 \text{ a}$	$68.4 \pm 1.9 \text{ b}$	73.9	9
4.33	108	$63.6 \pm 1.4 \text{ a}$	$71.0 \pm 0.9 \text{ c}$	72.9	9

\* When differences in methane content in biogas between control and nZVI reactors were significant ( $p < 0.05$ ).

97% cut-off, and resulting OTUs were phylogenetically classified to the maximum taxonomical level possible using the BLAST tool for Local Alignment (NCBI, <http://blast.ncbi.nlm.nih.gov/Blast.cgi>) and the associated GenBank database, as well as EzBioCloud 16S database.

Shared and unshared OTUs among samples were represented through Venn diagram, while biodiversity was estimated by calculating Shannon-Wiener, Chao 1 and Simpson indices at species taxonomic level ( $\alpha$ -biodiversity), using a 97% sequence similarity threshold for the establishment of OTUs. Sørensen-Dice qualitative (presence/absence data) and quantitative (relative abundance data) indices provided knowledge about community similarity among samples ( $\beta$ -biodiversity). Finally, evolutionary relationships between species were established using the Neighbor-Joining method with Mega version 6.0 software.

## 2.7. Statistical analysis

Statistical analysis was based on one-way ANOVA ( $p < 0.05$  confidence) with the Tukey test. Significant differences were analysed comparing nZVI reactors with control reactors (without nZVI) using the software Minitab 16 (Minitab Inc.). Values were reported as the average of replicates and the corresponding standard deviation.

## 3. Results and discussion

### 3.1. Overall performance of the reactors

The effect of nZVI addition was studied through the evolution of typical operational parameters. Data corresponding to pH, alkalinity and VFA are presented in Supplementary material. VS removal ranged between 50% and 60% for all the reactors, with small fluctuations due to substrate variability (Fig. S2). Some authors have reported an improvement in solid removal when nZVI were added, such as Córdova et al. (2019). The latter observed an increment on VS removal of 19.6% on batch AD experiments using sewage sludge. However, no statistical differences were found between nZVI and control group reactors for both sets of experiments in this work.

TA remained practically constant, and the IA/PA ratio remained lower than 0.5 for Experiment 1 and 0.3 for Experiment 2 without any significant differences between nZVI and control reactors. IA/PA ratios of 0.9 were suggested to maintain a total VFA below  $2.5 \text{ g L}^{-1}$  during the thermophilic AD of sewage sludge (Ferrer et al., 2010). In accordance, pH was reasonably constant in Experiment 1 ( $7.5 \pm 0.1$  and  $7.4 \pm 0.1$  for nZVI and control reactors, respectively) and Experiment 2 ( $8.0 \pm 0.1$  and  $7.9 \pm 0.1$ ). In agreement with the trend followed by alkalinity and pH, VFA remains low during all the operation for Experiment 1, being the highest reached value of  $0.22 \text{ g L}^{-1}$  (Fig. S3). The addition of nZVI has been previously related to the promotion of VFA production (Jia et al., 2017). Also, Feng et al. (2014) reported an increase of 37.3% of VFA after nZVI supplementation. Both studies were performed in batch; however, the trend of VFA observed in this work appeared not to be influenced by dosing nZVI tested in semi-continuous operation.

### 3.2. Effect of nZVI on biogas production and composition

Unexpectedly, and contrarily to most of the studies on this topic, biogas production was not statistically different when nZVI were added. Averaged biogas production rate was  $0.25 \pm 0.08$  for nZVI reactors and  $0.26 \pm 0.08 \text{ m}^3 \text{ biogas m}^{-3} \text{ d}^{-1}$  for control reactors in Experiment 1, and  $0.48 \pm 0.06$  and  $0.45 \pm 0.06 \text{ m}^3 \text{ biogas m}^{-3} \text{ d}^{-1}$  for Experiment 2 (nZVI and control reactors, respectively) (Fig. S4). Volumetric biogas production was in line with the obtained in Riu Sec WWTP,  $0.33 \text{ m}^3 \text{ biogas m}^{-3} \text{ d}^{-1}$  (personal communication). As stated above, biogas production improvement has been one of the most reported benefits of the use of nZVI. Jia et al. (2017) observed an increment in biogas

production of 18.1 but only 6.9% in the methane content. Su et al. (2013) reported improved production of biogas and methane by 30.4 and 40.4%, respectively. Nevertheless, all of the reported works dealing with the effects of nZVI in AD have been performed in batch conditions, which could be the reason behind the differences observed with this work.

#### 3.2.1. Biogas composition: methane enrichment after nZVI dosing

In Experiment 1, the first dose of  $0.27 \text{ g L}^{-1}$  of nZVI was supplemented on day 38. Immediately after the addition, methane content in biogas was statistically different ( $p < 0.05$ ) from the mean in control reactors (66.1%), reaching maximum methane content of 72.6% (Table 1). This effect was previously reported and attributed to several possible causes (Suanon et al., 2017). Low  $\text{CO}_2$  production has been related to the partial conversion of produced  $\text{CO}_2$  to methane via electron transfer. Also, the addition of nZVI could contribute to the production of  $\text{H}_2$  via the microbial corrosion and surface oxidation of nZVI and the produced  $\text{H}_2$  could directly be used by hydrogenotrophic methanogens to convert  $\text{CO}_2$  to  $\text{CH}_4$ . Also, homoacetogenic bacteria could use  $\text{CO}_2$  and overproduced  $\text{H}_2$  for the formation of acetate. Besides, Xu et al. (2019) reported that nZVI addition contributes to stable and favourable conditions for methanogens by lowering the oxidation–reduction potential. However, the effect was only sustained for some days after dosing, since there were no significant differences between the two groups of reactors six days after nZVI addition. Methane composition was monitored during one HRT before adding a new dose. No significant differences were observed between both groups of reactors during this time. The day 57, the next dose, doubling the first one ( $0.54 \text{ g L}^{-1}$ ), was added. Again, the difference between both groups of reactors started to be statically different immediately after the addition. In this case, the enhancement was significantly higher for seven days. The increase of methane in the biogas per day was similar for both doses (Table 1). After the addition of these two punctual doses, the results suggested that a minimum of freshly synthesized nZVI should remain in the reactor to enhance biogas composition. The loss of the effect could be attributed to changes in nZVI once in contact with the anaerobic medium, possibly related to their role as an electron donor (Dong et al., 2019) and possible oxidation.

#### 3.2.2. Dosing nZVI to sustain the positive effect over a long period

Four doses of  $0.27 \text{ g L}^{-1}$  were periodically added to the nZVI reactors every 5–7 days to evaluate if the methane content increase could be sustained in long-term operation. Results in Table 1 confirmed the viability to operate in semi-continuous mode, dosing nZVI every seven days to maintain the methane-enriched biogas. During these periods, an increase of 12.6% in methane content on average was observed compared to control reactors (Fig. 1a).

Lastly, after confirming that the effects persisted dosing of  $0.27 \text{ g L}^{-1}$  every seven days, the effect of a higher dose ( $0.81 \text{ g L}^{-1}$ ) was tested. In this case, methane content was increased from 65.1% to 75.9% (Table 1), with a maximum methane content of 78.6%. An averaged increment of 16.6% for four days was observed with respect to the control reactors. This increment was in accordance with Córdova et al. (2019), who observed an increase in methane content from 63.2% to 77.6%, and with Jia et al. (2017), who reported an increase of methane content of 6.93% in a batch test. Methane content in biogas for all Experiment 1 is shown in Fig. 1a. Biogas composition was always analysed before feeding the reactors. Only methane and  $\text{CO}_2$  were quantified while  $\text{H}_2$  was undetected.

#### 3.2.3. Dose-response effect on methane production

As observed in Experiment 1, increased methane in biogas was detected after the first dose of  $0.27 \text{ g L}^{-1}$  for five days in Experiment 2 (Fig. 1b). The next dose (doubling the first one) sustained the effects also for five more days (Table 1). The following doses (each doubling the previous one) lengthened the impact up to 9 days. Moreover, a

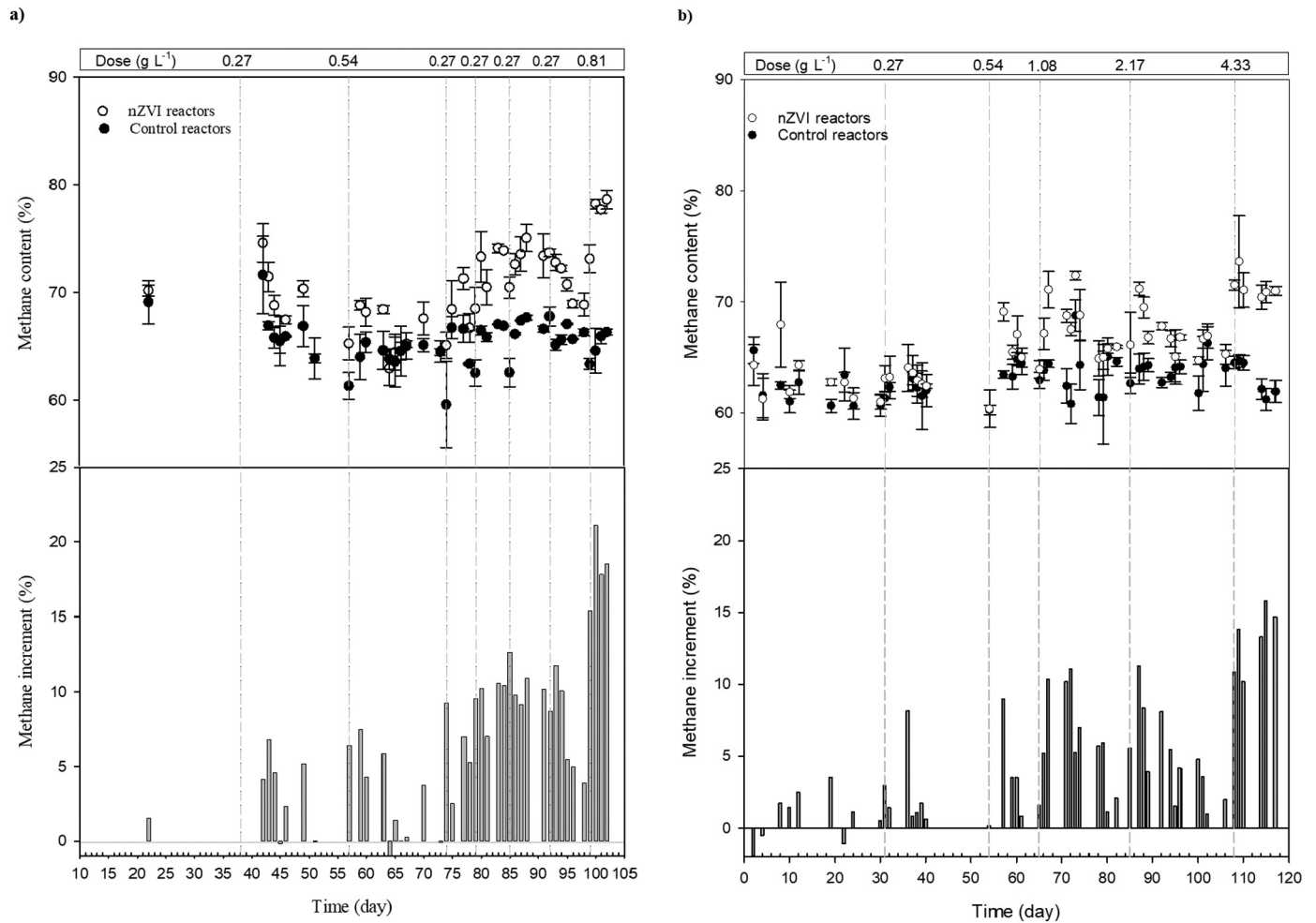


Fig. 1. Methane content in biogas for nZVI and control reactors; a) Experiment 1 and b) Experiment 2.

trend can be observed since the higher the dose the higher methane percentage was obtained on average (over the time that the effect persists).

Fig. 2 shows a boxplot with methane values from nZVI reactors for each dose. Only values statistically different ( $p < 0.05$ ) from control reactors were considered in the boxplot. Boxplot lengths showed that

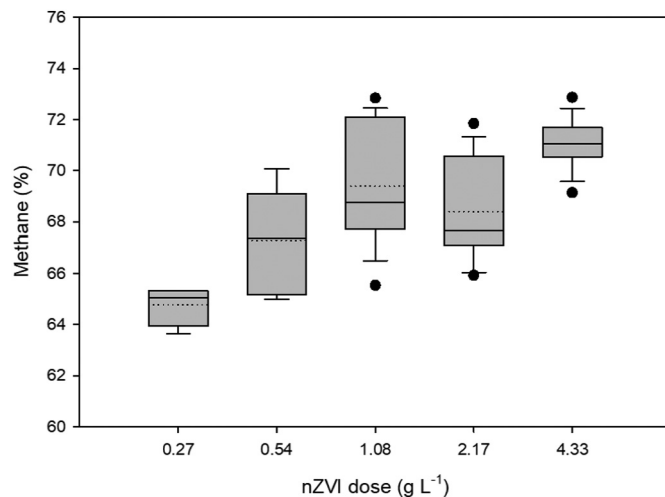


Fig. 2. Significantly improved methane values from nZVI reactors for each dose in Experiment 2. Dotted lines in boxplots indicate mean values.

data is skewed to the right for doses 1.08 and 2.17  $\text{g L}^{-1}$ . Values below the median were less dispersed for these doses, probably because of the higher frequency of high amounts of methane. Instead, high dispersion above the median (first dose) can be related to the fastest loss of effect after the addition. Only the highest dosage tested (4.33  $\text{g L}^{-1}$ ) could sustain the positive effect for more time in high values. Methane data was concentrated in a narrow range of values, being the highest of all doses tested. Accordingly, methane content was sustained for 9 days in the highest values, implying an important improvement in methane yield. Methane yield for this period was  $179 \pm 24$  and  $202 \pm 13$  for control and nZVI reactors respectively, reaching an increment of 12.7% in nZVI reactors.

Therefore, the results suggest that higher doses would result in better performance in long-term operation to achieve reliable improved yields. However, some authors have observed adverse effects when working with lower doses than the ones studied here. For instance, Yang et al. (2013) reported a reduction of 69% in methane production when 1.6  $\text{g L}^{-1}$  nZVI was used in batch experiments. Also, in batch experiments, Wang et al. (2018) established the optimum dosage at 1.0  $\text{g L}^{-1}$  because further addition could cause inhibition of methanogenesis step. In this sense, the gradual acclimation and adaptation of the microbiota after punctual doses raises as a hypothesis for the better performance of the process, as well as differences in the morphology and purity of the employed materials. As observed in Table 1, the same dose (0.27  $\text{g L}^{-1}$ ) did not show the same effect at day 3 when significant differences were found between them. In this sense, it should be interesting to study the effect of higher doses in a continuous operation mode using an acclimated microbial consortium having in mind the

possible changes that higher doses can have on microbial communities. Indeed, [Dong et al. \(2019\)](#), using  $25 \text{ g L}^{-1}$  of nZVI reported the promotion of homoacetogenesis, with acetic acid production instead of conversion of  $\text{CO}_2$  to  $\text{CH}_4$ , and inhibition of the methanogenesis, which is a dose significantly higher than the employed in this work.

The magnetic retention of nZVI in the reactors allowed showing the loss of its effect on methane content over time. This could be an important knowledge to operate in semi-continuous mode, avoiding the continuous nZVI addition and working efficiently without adding more nZVI than necessary. In this sense, the study of NPs properties once added to the reactors can help to understand the loss of efficiency over time and the mechanisms involved in the enhancement of AD.

### 3.3. Physical and chemical nZVI properties

#### 3.3.1. NPs morphology and size distribution after the anaerobic digestion process

[Fig. 3a](#) shows SEM images of nZVI before their addition to the anaerobic digesters. It can be observed how nZVI of sizes ranging from 10 to 30 nm tend to agglomerate. It has been previously reported that these NPs have a strong tendency to form microscale aggregates, likely due to the weak surface charges ([Sun et al., 2006](#); [Zhou et al., 2020](#)). This phenomenon could partially explain their loss of efficiency over time in the present study, as the contact surface is reduced as aggregation increases.

Regarding nZVI extracted from the digester at the end of the process (Experiment 1, day 99), in some areas of the sample, it is noted how the surface of nZVI can become scraggy and rough ([Fig. 3b](#)). [Zhen et al. \(2015\)](#) reported that many “flower-shaped” crystals made by prismatic iron (hydr)oxides clusters (e.g.,  $\text{FeCO}_3$ ,  $\text{Fe}_3\text{O}_4$ ,  $\text{Fe}(\text{OH})_3$  and  $\text{FeOOH}$ ) are found on the nZVI surface. [Fig. 3c](#), shows a representative image of a sample extracted from a reactor towards the end of the study (Experiment 1, day 99). It shows the presence of nZVI in the anaerobic digester, where these can be clearly identified by its spherical shape and scattered surface ([Fig. 3d](#)). An EDX analysis of this area revealed an iron composition of 78% in weight. It can be observed that nZVI are mixed with sludge, and they have not been washed off the reactor. In

[Fig. 3e](#) an image of a control reactor is shown, where sludge flocs displayed a rigid and compact structure, hallmark of a NPs free sludge.

The size of the NPs obtained is similar to that used by [Su et al. \(2013\)](#) who used the  $1 \text{ g L}^{-1}$  of commercial NPs (size 20 nm) and obtained 13.2% increase in the methane content of biogas. [Jia et al. \(2017\)](#), studied the effect of 50–70 nm NPs reaching an increase of 6.9% in the methane content of biogas using the same concentration of  $1 \text{ g L}^{-1}$ . As mentioned previously, in our study, the methane content was increased 16.6 and 11.6%, in Experiments 1 and 2, respectively. It has been reported different factors affecting nZVI effect on AD related to both nZVI particle characteristics (particle size, surface properties, dosage, etc.) but also microbial structure in the system ([Wang et al., 2018](#)). Special attention should be paid to phosphate concentration in the medium due to its high affinity with nZVI and other iron species. Phosphate can be easily adsorbed onto iron surface, which makes of it a good candidate for phosphate removal from aqueous solutions. One of the reported mechanisms for this affinity is that hydroxyl species are formed on iron surfaces, and this group is easily replaced by phosphate ([Wen et al., 2014](#)). Thus, this interaction can affect the process in two main ways: 1) modifying the surface structure and properties of nZVI, since adsorbed phosphate could combine with iron ions to form stable complexes, among which vivianite is one of the most common ([Wen et al., 2014](#)); and 2) affecting methanogenic activity since the aforementioned complexes could hinder the phosphorus uptake by methanogenic microorganisms ([Zhu et al., 2021](#)). Indeed, phosphate analysis should be necessary to really understand the efficiency of nZVI dosage in view to further experiments regarding dose optimization.

#### 3.3.2. Oxidation state after the anaerobic digestion process

TEM-EELS analysis was used to evaluate the oxidation state of iron at the beginning and the end of the studied processes. The most common procedure to assess the oxidation state of a metal is based on the  $L_{2,3}$  white-line ratio, which has a value of 2.99 for zero-valent iron, 3.99 for  $\text{Fe}^{2+}$  and 4.55 for  $\text{Fe}^{3+}$  ([Tan et al., 2012](#)). In the present case, nZVI revealed a 3.70 ratio at the beginning of the process, a value that increased up to 5.60 at the end. Thus, there is clear oxidation of the nZVI during the AD, confirming the electron donor capacity of nZVI ([Jia et al., 2017](#)).

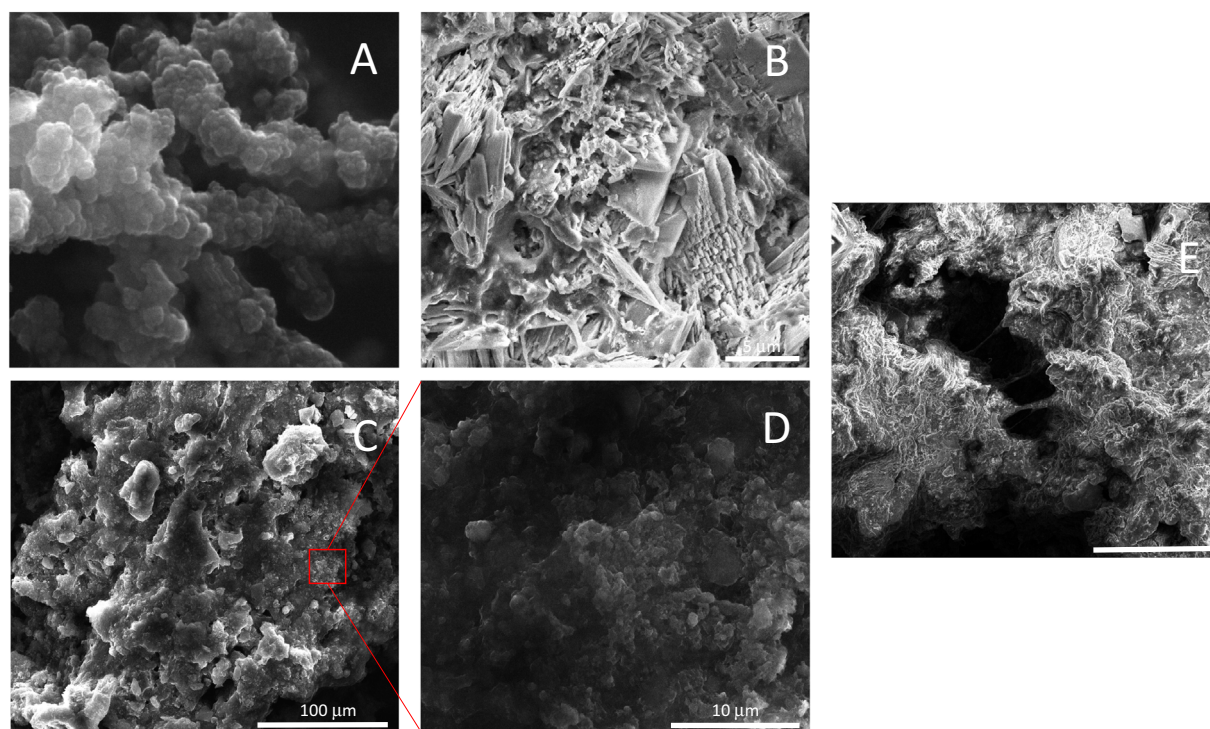


**Fig. 3.** SEM images of A) nZVI particles before being used for AD; B) and C) sample from nZVI reactors; D) Zoom picture of the indicated area of picture C; E) sample from control reactors.

Zhen et al. (2015) observed that the use of zero-valent scrap iron could offer electrons and promote H<sub>2</sub> as a source of electron donors for the AD of sewage sludge, accelerating different AD steps. Karri et al. (2005) indicated that Fe<sup>0</sup> could serve as a significant slow-release electron donor, noticing that Fe could directly be used for reducing CO<sub>2</sub> into CH<sub>4</sub> through autotrophic methanogenesis. So, the study of microbial community changes can also help understand how the oxidation of nZVI could be exploited for AD performance, understanding some of the involved mechanisms.

### 3.4. Effect of nZVI on microbial community

It is widely accepted that nZVI supplementation affects the structure of the indigenous microbial communities (Zhang et al., 2020). In some cases, such affectation has been described as negative to a greater or lesser extent (Xiu et al., 2010). On the contrary, methanogenic populations seem to respond positively to them (Antwi et al., 2017). At first sight, our results confirm the existence of alterations in the microbial community structure because of the application of nZVI. According to  $\alpha$ -biodiversity indices (Table 2), both processes can be considered as very rich and heterogeneous from a prokaryotic point of view, which corresponds well to the fact pointed out by other authors studying AD supplemented with Fe nanoparticles (Ambuchi, 2018). However,  $\beta$ -biodiversity Sørensen–Dice index revealed differences derived from the presence of nZVI, not associated to the identity of species but because of the relative abundance (>0.5%) of dominant bacteria. Fig. 4a shows the composition of the microbial community (phylum taxonomic level) at the end of the processes and Fig. 4b presents the percentage changes for each phylum in nZVI and control reactors. Most of the prokaryotic groups showed increased relative abundances when nZVI particles were added, especially Aminicenantes, Verrucomicrobia and Proteobacteria. Aminicenantes and Verrucomicrobia are not considered as common members of usual microbiome of AD and their presence, if so, can be termed as marginal (Calusinska et al., 2018). Considering the methanotrophic potential of some species assigned to Verrucomicrobia phylum (van Teeseling et al., 2014), their relatively low significance has a positive character. On the contrary, Proteobacteria are usually common members of the AD microbiome, and their stimulation on account of nZVI supplementation has already been reported in similar conditions (Wang et al., 2018). This can be assumed as positive since they are strongly related to the acidification process, which is essential for methanogens activity. A similar role can be assigned to the members of phyla Bacteroidetes and Cloacimonetes, for which the stimulating effect of nZVI was not as marked as in the case of Proteobacteria, although their relative abundances, between 13% and 20%, were far outstripping than those observed for Proteobacteria, never above 3%. Both microbial groups are significant microbiota members responsible for the hydrolysis of carbon compounds and further transformation into molecules that support methanogenic activity (Chojnacka et al., 2015). This is also the case of representatives of Thermotogae, a phylum integrated by microorganisms showing a close relation with members of Archaea, which are recognized H<sub>2</sub> producers (Bhandari and Gupta, 2014). The increase in their relative abundance in

nZVI reactors, from 4.36% to 6.01%, might enhance the activity of hydrogenotrophic methanogens.

Among the numerous OTUs without direct assignation stood out a group of five sequences related to no cultivated microorganisms affiliated to the division-level “candidate” phylogenetic group WS6 (Table S1, supporting material). Such species are mostly associated with anaerobic environments including AD (Qiao et al., 2013) and have been described as capable of producing acetate, lactate and/or hydrogen (Wrighton et al., 2016). Moreover, some members of this clade carry genes encoding RuBisCO forms specific to Archaea (Hernsdorf et al., 2017). These characteristics emphasize their importance in methanogenic processes and explain their high relative abundance, the third most dominant group, in both reactors. Data about the influence of nZVI on representatives of WS6 group is practically non-existent, although the limited information available regarding anaerobic processes suggests a slight positive effect (Zhang et al., 2018; Xiang et al., 2019).

The most dominant phylum, both in the absence and in the presence of nZVI, was Firmicutes. All of the dominant OTUs assigned to this phylum belong to Clostridia class, which is expected since members of this class are close associates to AD and methanogenesis because of their ability to produce different substrates that promote methanogenic activity (Dos Reis et al., 2015). The relative abundance of Firmicutes decrease in nZVI reactors, 20.59%, in comparison to control, 30.76%. Results are contradictory concerning this phylum, since some studies report a positive effect of nZVI supplementation (Antwi et al., 2017; He et al., 2017), but many others describe a decrease in the quantitative presence of their representatives (Pan et al., 2017; Zhang et al., 2018). Iron can play a dual role regarding viability of microbial cells, a positive one associated to its nutritional function, and a negative one derived from the production of reactive oxygen species that strongly affect cell membranes (Daraei et al., 2019), and promote disruption of cell integrity (Yang et al., 2013). Indeed, oxidation of nZVI is responsible for both, to act as co-factor (co-reducer) to promote the conversion of CO<sub>2</sub> into CH<sub>4</sub>, or, by the same mechanisms, the generation of toxic free radicals. Consequently, nZVI need to be carefully introduced into the AD processes. Besides, the prevalence of one or another effect and, in consequence, the response of specific microorganisms, will be mostly depending on environment (Kong et al., 2018).

A more detailed analysis of the direction of the changes taking place in Firmicutes at species level (Fig. 5) revealed decreases in *Sedimentibacter* and *Syntrophomonas* representatives, as well as OTU 6892, affiliated to Peptococcaceae family (Accession number LT625357.1), and an increase in OTU 18225, also identified as a member of the Clostridia group. Clostridia are considered one of the most significant communities integrating the so-called core microbiome in AD (De Vrieze et al., 2016). Species belonging to Clostridium, *Sedimentibacter*, and *Syntrophomonas* have been recognized as prevalent OTUs within this core microbiome. However, the dominance of one or other is conditioned by both nutritional and environmental parameters (Rui et al., 2015). In this sense, the point is the maintenance of the community overall functionality to provide the substrates needed for the methanogenic activity (Treu et al., 2016). The balance between the main types of substrates, in turn, determines which methanogenic community, acetotrophic or hydrogenotrophic, will lead the process.

The methanogenic community remained stable in both reactors (Fig. 6), with the only exception of species assigned to *Methanotrux* genus, which increased their relative abundance from 0.2% in control up to 0.57% in nZVI reactors. Members of this genus are recognized as specialist methanogenic bacteria that only use acetate for their growth (Stams et al., 2019), a substrate for which they have greater affinity than other acetoclastic species (Smith and Ingram-Smith, 2007). This greater affinity could explain its marked rise, as it has been suggested by other studies (Röske et al., 2014), since it would be reasonable to expect that acetate concentration in nZVI reactors is lower because of the reduction in the relative abundances of acetate-producer bacteria, such as *Sedimentibacter*, or *Syntrophomonas* (Breitenstein et al., 2002; Kong et al., 2018). The higher relative abundance of other acetate-

**Table 2**

$\alpha$ - and  $\beta$ -biodiversity estimated according to Shannon–Wiener, Chao 1 and Simpson and Sørensen–Dice qualitative and quantitative indices, respectively. The last one was calculated for both the whole community and the dominant community (relative abundance >0.5%). Indices were calculated at species taxonomic level.

Index	Control	nZVI
Shannon–Wiener richness index	4.43	4.48
Chao 1 estimator of total richness	1891	1712
Simpson dominance index	0.04	0.04
Sørensen–dice qualitative index	Absolute	>0.5%
	nZVI 0.64	0.97
Sørensen–dice quantitative index		
	nZVI 0.71	0.74

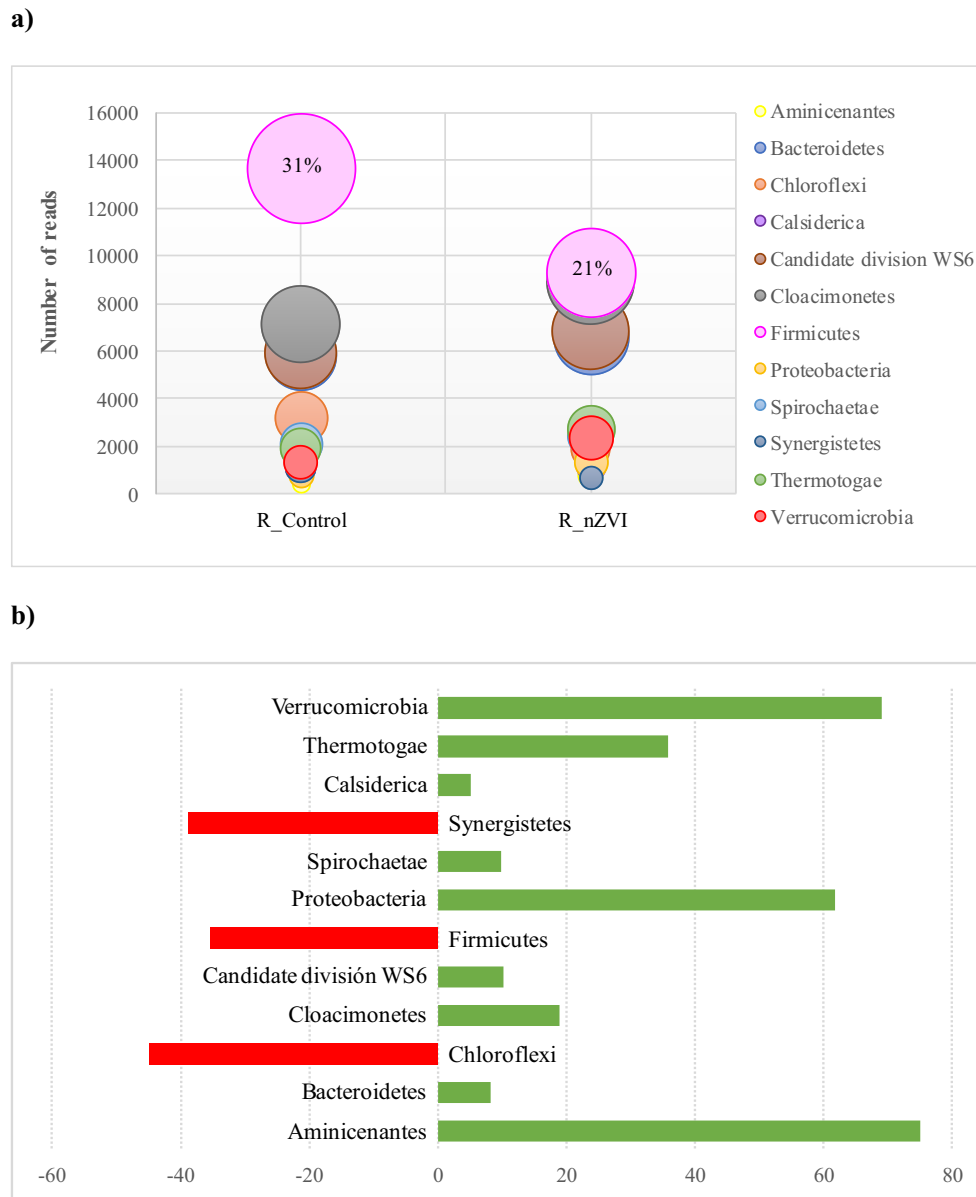


**Fig. 4.** a) Number of reads and relative importance of the prevalent OTUs (relative abundance >0.5%) in both samples at phylum taxonomic level. Relative importance within the sample is expressed as bubble size (diameter). Data for maximum abundances are included in respective bubbles as a reference. b) Percentage changes in phyla relative abundances among prevalent OTUs representing both microbiomes. Green color means higher abundance in nZVI reactors and red color in control reactors.

producer species, like those assigned to Cloacimonetes taxon or Porphyromonadaceae family (OTU 7658) (Esquivel-Elizondo et al., 2016; Hahnke et al., 2015) appears not to be sufficient to maintain the same level as in control reactors but enough to assure the prevalence of acetotrophic pathway over hydrogenotrophic methanogenesis. The increased presence of some  $H_2$ -producers, as in the case of OTU 18825 assigned to *Hydrogenospora* genus (Azizi et al., 2016), have been previously reported in AD supplemented of nZVI (Huang et al., 2019). This result might suggest a larger contribution of hydrogenotrophic processes for the production of methane. However, it has been recently reported that its activity could be associated to  $H_2$  consumption rather than  $H_2$  production (Zhu et al., 2019), which would be consistent with results here described. On the other side, a recent study reveals the isolation of a methanogen that clusters with *Methanotherix* and shows hydrogenotrophic activity (Blesy et al., 2019). Further and more extensive studies will be necessary to establish the existence of one or another option, or even the co-existence of both of them.

#### 4. Conclusions

Dossing a few  $g L^{-1}$  zero-valent iron nanoparticles (nZVI) every 5–7 days could be a successful strategy in the semi-continuous anaerobic digestion of sewage sludge to enhance methane content in biogas (16.6%) and sustain it over time, avoiding the continuous addition of nZVI. The acclimatization of the microbial community seems to be an important step to the efficient use of nZVI. According to the structure of prokaryotic communities, acetotrophic methanogenesis seems to be the prevalent via in both reactors, although the supplementation with nZVI altered the balance among acetogenic eubacteria and stimulated the presence of apparently  $H_2$ -producer species. *Methanotherix*, an acetoclastic archaea showing high acetate affinity, was strongly encouraged by nZVI, which sustain the dominance of acetotrophic processes. In any case, further research is needed the study the effects of nZVI accumulation in the reactors in a long-term operation once their oxidation occurs and contemplating recovery and reuse options. Dose



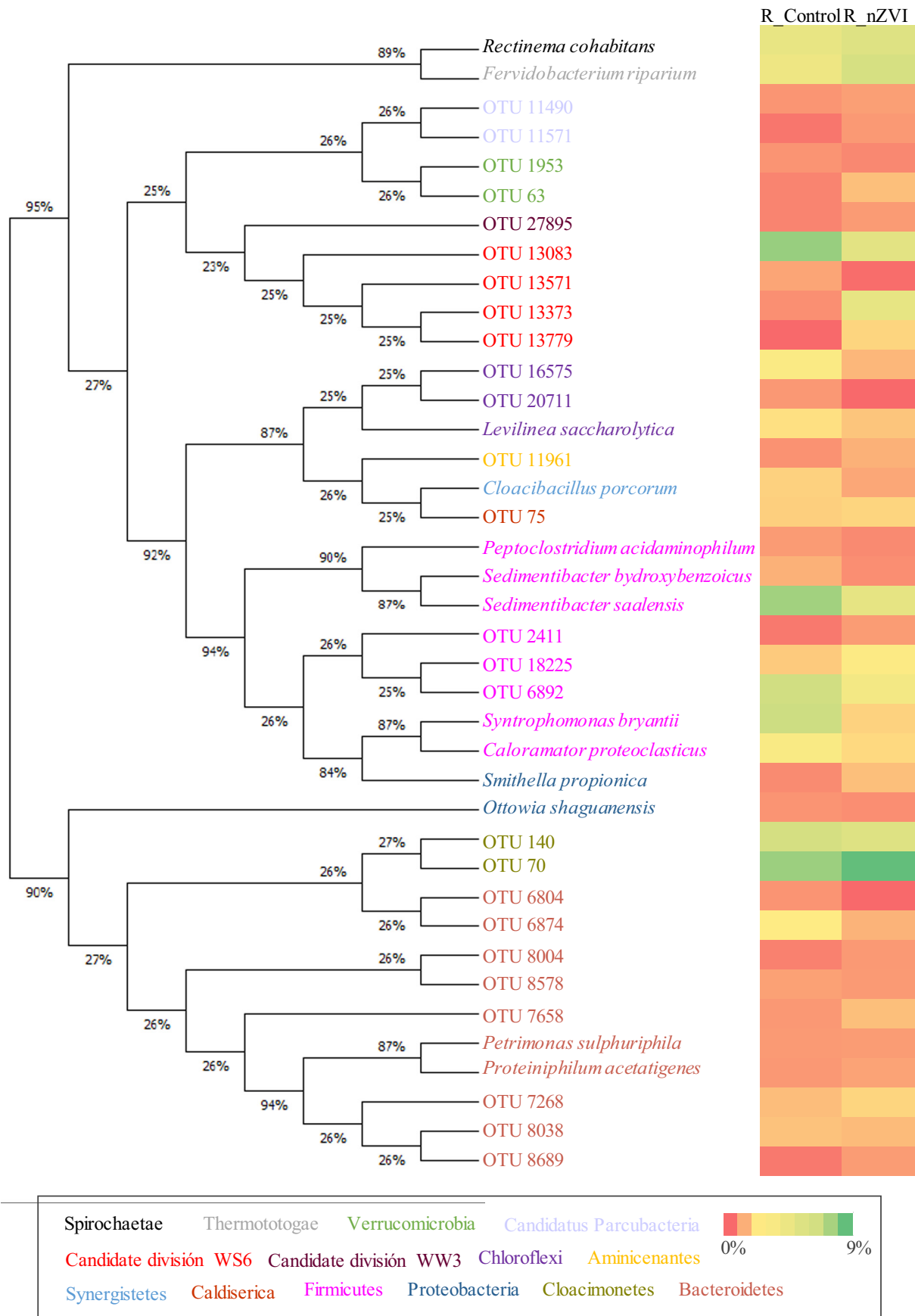


**Fig. 5.** Evolutionary history, inferred from rRNA 16S gene sequences associated to prevalent OTUs (relative abundance >0.5%) in at least one of the samples, and corresponding heatmap. The tree was constructed using the Neighbor-Joining method and the p-distance method for computing the evolutionary distances.

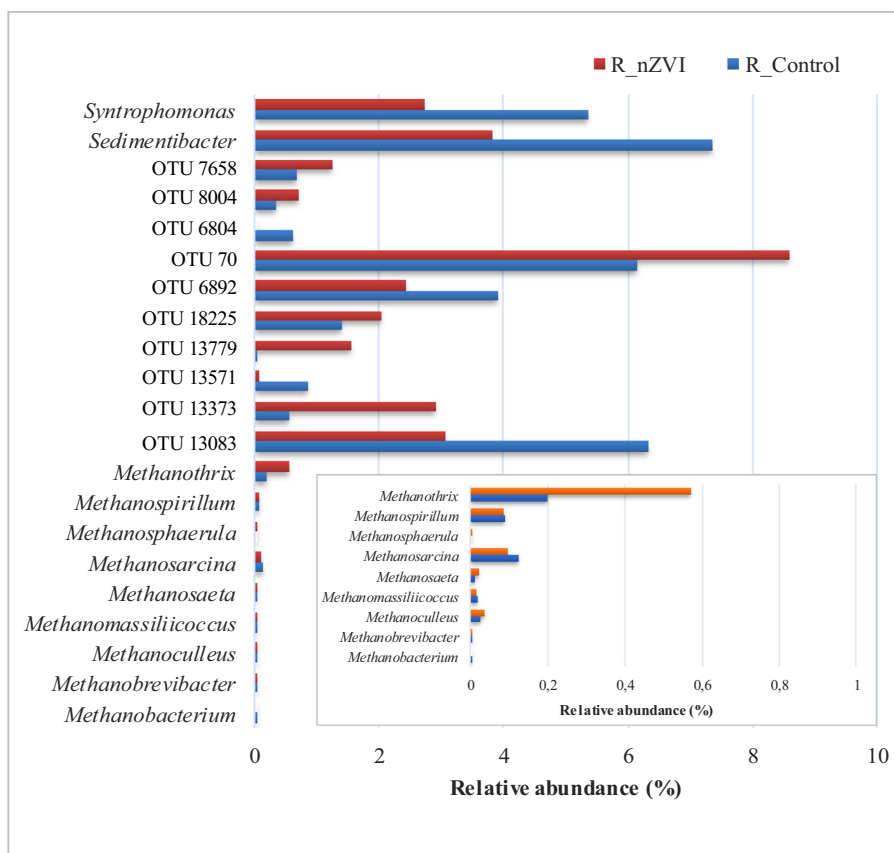


Fig. 6. Relative abundance of methanogens and more significant eubacteria to methanogenic activity.

optimization should also be tackled to operate efficiently in a semi-continuous mode without adding more nZVI than necessary and considering phosphate interactions with iron ions. Further consideration should be given to the quality of digestate in order to avoid any problem related to its valorisation. An enrichment methane streams of biogas in sewage sludge anaerobic digestion could be an interesting alternative facilitating the upgrading of biogas.

#### CRedit authorship contribution statement

**Raquel Barrena:** Conceptualization, Visualization, Writing – original draft. **María del Carmen Vargas-García:** Formal analysis, Writing – original draft. **Georgina Capell:** Investigation, Validation. **Maja Barańska:** Investigation, Validation. **Victor Puentes:** Writing – review & editing. **Javier Moral-Vico:** Conceptualization, Investigation, Writing – original draft. **Antoni Sánchez:** Conceptualization, Writing – review & editing. **Xavier Font:** Conceptualization, Writing – review & editing.

#### Declaration of competing interest

The authors declare that they have no known competing financial interests or personal relationships that could have appeared to influence the work reported in this paper.

#### Acknowledgments

The authors thank EDAR Sabadell Riu SEC for the provision of sewage sludge and inoculum. Raquel Barrena is grateful to TECNIOspring fellowship programme (TECSPR15-1-0051) co-financed by the European Union through the Marie Curie Actions and ACCIÓ (Generalitat de Catalunya).

#### Appendix A. Supplementary data

Supplementary data to this article can be found online at <https://doi.org/10.1016/j.scitotenv.2021.145969>.

#### References

- Ambuchi, J.J., 2018. Hematite and multi-walled carbon nanotubes stimulate a faster syntrophic pathway during methanogenic beet sugar industrial wastewater degradation. *Appl. Microbiol.* 102, 7147.
- Antwi, P., Li, J., Boadi, P.O., Meng, J., Shi, E., Chi, X., Deng, K., Ayivi, F., 2017. Dosing effect of zero valent iron (ZVI) on bioremediation and microbial community distribution as revealed by 16S rRNA high-throughput sequencing. *Int. Biodeterior. Biodegrad.* 123, 191–199. <https://doi.org/10.1016/j.ibiod.2017.06.022>.
- APHA, 1999. Standard methods for the examination of water and wastewater standard methods for the examination of water and wastewater. *Public Health* <https://doi.org/10.2105/AJPH.51.6.940-a>.
- Azizi, A., Kim, W., Lee, J.H., 2016. Comparison of microbial communities during the anaerobic digestion of *Gracilaria* under mesophilic and thermophilic conditions. *World J. Microbiol. Biotechnol.* 32. <https://doi.org/10.1007/s11274-016-2112-6>.
- Baniamerian, H., Isfahani, P.G., Tsapekos, P., Alvarado-Morales, M., Shahrokhii, M., Vossoughi, M., Angelidaki, I., 2019. Application of nano-structured materials in anaerobic digestion: current status and perspectives. *Chemosphere* 229, 188–199. <https://doi.org/10.1016/j.chemosphere.2019.04.193>.
- Bhandari, V., Gupta, R.S., 2014. The phylum thermotogae. In: Rosenberg, E., DeLong, E.F., Lory, S., Stackebrandt, E., Thompson, F. (Eds.), *The Prokaryotes: Other Major Lineages of Bacteria and the Archaea*. Springer, Berlin Heidelberg, Berlin, Heidelberg, pp. 989–1015 [https://doi.org/10.1007/978-3-642-38954-2\\_118](https://doi.org/10.1007/978-3-642-38954-2_118).
- Blesy, G., Balachandar, D., Parwin Banu, K.S., Karthikeyan, S., 2019. Hydrogenotrophic activity of strain RWL1 similar to *Methanothrix soehngenii*. *Madras Agric. J.* 106, 624. doi:10.29321/maj.2019.000310
- Breitenstein, A., Wiegel, J., Haertig, C., Weiss, N., Andreesen, J.R., Lechner, U., 2002. Reclassification of *Clostridium hydroxybenzoicum* as *Sedimentibacter hydroxybenzoicus* gen. nov., comb. nov., and description of *Sedimentibacter saalensis* sp. nov. *Int. J. Syst. Evol. Microbiol.* 52, 801–807. <https://doi.org/10.1099/ij.s.0.01998-0>.

- Calusinska, M., Goux, X., Fossépré, M., Muller, E.E.L., Wilmes, P., Delfosse, P., 2018. A year of monitoring 20 mesophilic full-scale bioreactors reveals the existence of stable but different core microbiomes in bio-waste and wastewater anaerobic digestion systems. *Biotechnol. Biofuels* 11, 1. <https://doi.org/10.1186/s13068-018-1195-8>.
- Casals, E., Barrena, R., García, A., González, E., Delgado, L., Busquets-Fité, M., Font, X., Arbiol, J., Glatzel, P., Kvashnina, K., Sánchez, A., Puentes, V., 2014. Programmed iron oxide nanoparticles disintegration in anaerobic digesters boosts biogas production. *Small* 10. doi:<https://doi.org/10.1002/sml.201303703>.
- Choe, S., Lee, S.H., Chang, Y.Y., Hwang, K.Y., Khim, J., 2001. Rapid reductive destruction of hazardous organic compounds by nanoscale Fe<sub>0</sub>. *Chemosphere* 42, 367–372. [https://doi.org/10.1016/S0045-6535\(00\)00147-8](https://doi.org/10.1016/S0045-6535(00)00147-8).
- Chojnacka, A., Szczesny, P., Błaszczyk, M.K., Zielenkiewicz, U., Detman, A., Salamon, A., Sikora, A., 2015. Noteworthy facts about a methane-producing microbial community processing acidic effluent from sugar beet molasses fermentation. *PLoS One* 10, 1. <https://doi.org/10.1371/journal.pone.0128008>.
- Córdova, A., Carrera, C., Zepeda, A., Enrique, J., 2019. Enhancing the performance and stability of the anaerobic digestion of sewage sludge by zero valent iron nanoparticles dosage. *Bioresour. Technol.* 275, 352–359. <https://doi.org/10.1016/j.biortech.2018.12.086>.
- Daraei, H., Rafiee, M., Yazdanbakhsh, A.R., Amoozgar, M.A., Guanglei, Q., 2019. A comparative study on the toxicity of nano zero valent iron (nZVI) on aerobic granular sludge and flocculent activated sludge: reactor performance, microbial behavior, and mechanism of toxicity. *Process. Saf. Environ. Prot.* 129, 238–248. <https://doi.org/10.1016/j.psep.2019.07.011>.
- De Vrieze, J., Raport, L., Roume, H., Vilchez-Vargas, R., Jáuregui, R., Pieper, D.H., Boon, N., 2016. The full-scale anaerobic digestion microbiome is represented by specific marker populations. *Water Res.* 104, 101–110. <https://doi.org/10.1016/j.watres.2016.08.008>.
- Dong, D., Aleta, P., Zhao, X., Choi, O.K., Kim, S., Lee, J.W., 2019. Effects of nanoscale zero valent iron (nZVI) concentration on the biochemical conversion of gaseous carbon dioxide (CO<sub>2</sub>) into methane (CH<sub>4</sub>). *Bioresour. Technol.* 275, 314–320. <https://doi.org/10.1016/j.biortech.2018.12.075>.
- Dos Reis, C.M., Carosia, M.F., Sakamoto, I.K., Amâncio Varesche, M.B., Silva, E.L., 2015. Evaluation of hydrogen and methane production from sugarcane vinasse in an anaerobic fluidized bed reactor. *Int. J. Hydrogen Energy* 40, 8498–8509. <https://doi.org/10.1016/j.ijhydene.2015.04.136>.
- Edgar, R.C., Haas, B.J., Clemente, J.C., Quince, C., Knight, R., 2011. UCHIME improves sensitivity and speed of chimera detection. *Bioinformatics* 27, 2194–2200. <https://doi.org/10.1093/bioinformatics/btr381>.
- Esquivel-Elizondo, S., Parameswaran, P., Delgado, A.G., Maldonado, J., Rittmann, B.E., Krajmalnik-Brown, R., 2016. Archaea and bacteria acclimate to high total ammonia in a methanogenic reactor treating swine waste. *Archaea* 2016. <https://doi.org/10.1155/2016/4089684>.
- Feng, Y., Zhang, Y., Quan, X., Chen, S., 2014. Enhanced anaerobic digestion of waste activated sludge digestion by the addition of zero valent iron. *Water Res.* 52, 242–250. <https://doi.org/10.1016/j.watres.2013.10.072>.
- Ferrer, I., Vázquez, F., Font, X., 2010. Long term operation of a thermophilic anaerobic reactor: process stability and efficiency at decreasing sludge retention time. *Bioresour. Technol.* 101, 2972–2980. <https://doi.org/10.1016/j.biortech.2009.12.006>.
- Folgosa, F., Tavares, P., Pereira, A.S., 2015. Iron management and production of electricity by microorganisms. *Appl. Microbiol. Biotechnol.* 99, 8329–8336. <https://doi.org/10.1007/s00253-015-6897-2>.
- Hahnke, S., Maus, I., Wibberg, D., Tomazetto, G., Pühler, A., Klocke, M., Schlüter, A., 2015. Complete genome sequence of the novel Porphyromonadaceae bacterium strain ING2-ESB isolated from a mesophilic lab-scale biogas reactor. *J. Biotechnol.* 193, 34–36. <https://doi.org/10.1016/j.jbiotec.2014.11.010>.
- He, C.S., He, P.P., Yang, H.Y., Li, L.L., Lin, Y., Mu, Y., Yu, H.Q., 2017. Impact of zero-valent iron nanoparticles on the activity of anaerobic granular sludge: from macroscopic to microcosmic investigation. *Water Res.* 127, 32–40. <https://doi.org/10.1016/j.watres.2017.09.061>.
- Hernsdorf, A.W., Amano, Y., Miyakawa, K., Ise, K., Suzuki, Y., Anantharaman, K., Probst, A., Burstein, D., Thomas, B.C., Banfield, J.F., 2017. Potential for microbial H<sub>2</sub> and metal transformations associated with novel bacteria and archaea in deep terrestrial subsurface sediments. *ISME J.* 11, 1915–1929. <https://doi.org/10.1038/ismej.2017.39>.
- Huang, Weiwei, Yang, F., Huang, Wenli, Wang, D., Lei, Z., Zhang, Z., 2019. Weak magnetic field significantly enhances methane production from a digester supplemented with zero valent iron. *Bioresour. Technol.* 282, 202–210. <https://doi.org/10.1016/j.biortech.2019.03.013>.
- Jia, T., Wang, Z., Shan, H., Liu, Y., Gong, L., 2017. Effect of nanoscale zero-valent iron on sludge anaerobic digestion. *Resour. Conserv. Recycl.* 127, 190–195. <https://doi.org/10.1016/j.resconrec.2017.09.007>.
- Karri, S., Sierra-Alvarez, R., Field, J.A., 2005. Zero valent iron as an electron-donor for methanogenesis and sulfate reduction in anaerobic sludge. *Biotechnol. Bioeng.* 92, 810–819. <https://doi.org/10.1002/bit.20623>.
- Kong, X., Yu, S., Fang, W., Liu, J., Li, H., 2018. Enhancing syntrophic associations among *Clostridium butyricum*, *Syntrophomonas* and two types of methanogen by zero valent iron in an anaerobic assay with a high organic loading. *Bioresour. Technol.* 257, 181–191. <https://doi.org/10.1016/j.biortech.2018.02.088>.
- Lora Grando, R., de Souza Antune, A.M., da Fonseca, F.V., Sánchez, A., Barrena, R., Font, X., 2017. Technology overview of biogas production in anaerobic digestion plants: a European evaluation of research and development. *Renew. Sust. Energ. Rev.* 80, 44–53. <https://doi.org/10.1016/j.rser.2017.05.079>.
- Pan, F., Zhong, X., Xia, D., Yin, X., Li, F., Zhao, D., Ji, H., Liu, W., 2017. Nanoscale zero-valent iron/persulfate enhanced upflow anaerobic sludge blanket reactor for dye removal: insight into microbial metabolism and microbial community. *Sci. Rep.* 7. <https://doi.org/10.1038/srep44626>.
- Qiao, J.T., Qiu, Y.L., Yuan, X.Z., Shi, X.S., Xu, X.H., Guo, R.B., 2013. Molecular characterization of bacterial and archaeal communities in a full-scale anaerobic reactor treating corn straw. *Bioresour. Technol.* 143, 512–518. <https://doi.org/10.1016/j.biortech.2013.06.014>.
- Röske, I., Sabra, W., Nacke, H., Daniel, R., Zeng, A.P., Antranikian, G., Sahn, K., 2014. Microbial community composition and dynamics in high-temperature biogas reactors using industrial bioethanol waste as substrate. *Appl. Microbiol. Biotechnol.* 98, 9095–9106. <https://doi.org/10.1007/s00253-014-5906-1>.
- Rui, L., Li, J., Zhang, S., Yan, X., Wang, Y., Li, X., 2015. The core populations and co-occurrence patterns of prokaryotic communities in household biogas digesters. *Biotechnol. Biofuels* 8, 1–15. <https://doi.org/10.1186/s13068-015-0339-3>.
- Smith, K.S., Ingram-Smith, C., 2007. Methanosaeta, the forgotten methanogen? *Trends Microbiol.* <https://doi.org/10.1016/j.tim.2007.02.002>.
- Stams, A.J.M., Teusink, B., Sousa, D.Z., 2019. Ecophysiology of acetoclastic methanogens. In: Stams, A.J.M., Sousa, D. (Eds.), *Biogenesis of Hydrocarbons*. Springer International Publishing, Cham, pp. 1–14. [https://doi.org/10.1007/978-3-319-53114-4\\_21-1](https://doi.org/10.1007/978-3-319-53114-4_21-1).
- Su, L., Shi, X., Guo, G., Zhao, A., Zhao, Y., 2013. Stabilization of sewage sludge in the presence of nanoscale zero-valent iron (nZVI): abatement of odor and improvement of biogas production. *J. Mater. Cycles Waste Manag.* 15, 461–468. <https://doi.org/10.1007/s10163-013-0150-9>.
- Suanon, F., Sun, Q., Li, M., Cai, X., Zhang, Y., Yan, Y., Yu, C.P., 2017. Application of nanoscale zero valent iron and iron powder during sludge anaerobic digestion: impact on methane yield and pharmaceutical and personal care products degradation. *J. Hazard. Mater.* 321, 47–53. <https://doi.org/10.1016/j.jhazmat.2016.08.076>.
- Sun, Y.P., Li, X., Qin, C., Cao, J., Zhang, W., Xian, W., Wang, H.P., 2006. Characterization of zero-valent iron nanoparticles. *Adv. Colloid Interf. Sci.* 120, 47–56. <https://doi.org/10.1016/j.cis.2006.03.001>.
- Takahashi, S., Tomita, J., Nishioka, K., Hisada, T., Nishijima, M., 2014. Development of a prokaryotic universal primer for simultaneous analysis of Bacteria and Archaea using next-generation sequencing. *PLoS One* 9, e105592. <https://doi.org/10.1371/journal.pone.0105592>.
- Tan, H., Verbeeck, J., Abakumov, A., Van Tendeloo, G., 2012. Oxidation state and chemical shift investigation in transition metal oxides by EELS. *Ultramicroscopy* 116, 24–33. <https://doi.org/10.1016/j.ultramic.2012.03.002>.
- Treu, L., Kougias, P.G., Campanaro, S., Bassani, I., Angelidaki, I., 2016. Deeper insight into the structure of the anaerobic digestion microbial community; the biogas microbiome database is expanded with 157 new genomes. *Bioresour. Technol.* 216, 260–266. <https://doi.org/10.1016/j.biortech.2016.05.081>.
- van Teeseling, M.C.F., Pol, A., Harhangi, H.R., van der Zwart, S., Jetten, M.S.M., Op den Camp, H.J.M., van Niftrik, L., 2014. Expanding the verrucomicrobial methanotrophic world: Description of three novel species of *Methylacidimicrobium* gen. nov. *Appl. Environ. Microbiol.* 80, 6782–6791. <https://doi.org/10.1128/AEM.01838-14>.
- Wang, Y., Wang, D., Fang, H., 2018. Comparison of enhancement of anaerobic digestion of waste activated sludge through adding nano-zero valent iron and zero valent iron. *RSC Adv.* 8, 27181–27190. <https://doi.org/10.1039/c8ra05369c>.
- Wen, Z., Zhang, Y., Dai, C., 2014. Removal of phosphate from aqueous solution using nanoscale zerovalent iron (nZVI). *Colloids Surfaces A Physicochem. Eng. Asp.* 457, 433–440. <https://doi.org/10.1016/j.colsurfa.2014.06.017>.
- Wrighton, K.C., Castelle, C.J., Varaljay, V.A., Satagopan, S., Brown, C.T., Wilkins, M.J., Thomas, B.C., Sharon, I., Williams, K.H., Tabita, F.R., Banfield, J.F., 2016. RubisCO of a nucleoside pathway known from Archaea is found in diverse uncultivated phyla in bacteria. *ISME J.* 10, 2702–2714. <https://doi.org/10.1038/ismej.2016.53>.
- Xiang, Y., Yang, Z., Zhang, Y., Xu, R., Zheng, Y., Hu, J., Li, X., Jia, M., Xiong, W., Cao, J., 2019. Influence of nanoscale zero-valent iron and magnetite nanoparticles on anaerobic digestion performance and macrofide, aminoglycoside, β-lactam resistance genes reduction. *Bioresour. Technol.* 294, 122139. <https://doi.org/10.1016/j.biortech.2019.12.139>.
- Xiu, Ming, Z., Jin, Z., Hui, Li, T., Long, Mahendra, S., Lowry, G.V., Alvarez, P.J.J., 2010. Effects of nano-scale zero-valent iron particles on a mixed culture dechlorinating trichloroethylene. *Bioresour. Technol.* 101, 1141–1146. <https://doi.org/10.1016/j.biortech.2009.09.057>.
- Xu, R., Xu, S., Zhang, L., Florentino, A.P., Yang, Z., Liu, Y., 2019. Impact of zero valent iron on blackwater anaerobic digestion. *Bioresour. Technol.* 285, 121351. <https://doi.org/10.1016/j.biortech.2019.12.1351>.
- Yang, Y., Guo, J., Hu, Z., 2013. Impact of nano zero valent iron (NZVI) on methanogenic activity and population dynamics in anaerobic digestion. *Water Res.* 47, 6790–6800. <https://doi.org/10.1016/j.watres.2013.09.012>.
- Zhang, Z., Gao, P., Cheng, J., Liu, G., Zhang, X., Feng, Y., 2018. Enhancing anaerobic digestion and methane production of tetracycline wastewater in EGSB reactor with GAC/NZVI mediator. *Water Res.* 136, 54–63. <https://doi.org/10.1016/j.watres.2018.02.025>.
- Zhang, Y., Xu, R., Xiang, Y., Lu, Y., Jia, M., Huang, J., Xu, Z., Cao, J., Xiong, W., Yang, Z., 2020. Addition of nanoparticles increases the abundance of mobile genetic elements and changes microbial community in the sludge anaerobic digestion system. *J. Hazard. Mater.* 124206. <https://doi.org/10.1016/j.jhazmat.2020.124206>.
- Zhen, G., Lu, X., Li, Y.Y., Liu, Y., Zhao, Y., 2015. Influence of zero valent scrap iron (ZVSI) supply on methane production from waste activated sludge. *Chem. Eng. J.* 263, 461–470. <https://doi.org/10.1016/j.cej.2014.11.003>.
- Zhou, J., You, X., Niu, B., Yang, X., Gong, L., Zhou, Y., Wang, J., Zhang, H., 2020. Enhancement of methanogenic activity in anaerobic digestion of high solids sludge

- by nano zero-valent iron. *Sci. Total Environ.* 703. <https://doi.org/10.1016/j.scitotenv.2019.135532>.
- Zhou, H., Cao, Z., Zhang, M., Ying, Z., Ma, L., 2021. Zero-valent iron enhanced in-situ advanced anaerobic digestion for the removal of antibiotics and antibiotic resistance genes in sewage sludge. *Sci. Total Environ.* 754, 142077. <https://doi.org/10.1016/j.scitotenv.2020.142077>.
- Zhu, X., Cao, Q., Chen, Y., Sun, X., Liu, X., Li, D., 2019. Effects of mixing and sodium formate on thermophilic in-situ biogas upgrading by H<sub>2</sub> addition. *J. Clean. Prod.* 216, 373–381. <https://doi.org/10.1016/j.jclepro.2019.01.245>.
- Zhu, X., Blanco, E., Bhatti, M., Borrion, A., 2021. Impact of metallic nanoparticles on anaerobic digestion: a systematic review. *Sci. Total Environ.* 757, 143747. <https://doi.org/10.1016/j.scitotenv.2020.143747>.